Brain Structure and Function (2019) 224:435–452
https://doi.org/10.1007/s00429-018-1781-3

ORIGINAL ARTICLE

Meta-analysis of functional subdivisions within human posteromedial cortex

Yuefeng Huang[1] · Jeffrey Hullfish[1] · Dirk De Ridder[2] · Sven Vanneste[1]

Received: 5 July 2018 / Accepted: 17 October 2018 / Published online: 26 October 2018

Abstract

The posteromedial cortex (PMC)—comprising posterior cingulate cortex (PCC), retrosplenial cortex (RSC), and the precuneus (PrC)—is perhaps best known for its involvement in the default mode network. There is no consensus regarding the specific functions of PMC, however, and its component regions each exhibit distinct, but partially overlapping functional profiles. To date, there has been minimal effort to disentangle the functions of these regions. In the present study, we use Neurosynth (http://neurosynth.org) to conduct an unbiased meta-analysis of the PMC based on fMRI coactivation and semantic information extracted from 11,406 studies. Our analyses revealed six PMC clusters with distinct functional profiles: superior and inferior dorsal PCC, anterior and posterior PrC, ventral PCC, and RSC. We discuss these findings in the context of the existing literature and suggest several fruitful avenues for continued research.

Keywords Default mode network · Posterior cingulate cortex · Precuneus · Retrosplenial cortex

Introduction

Posteromedial cortex (PMC) refers to the part of cerebral cortex located in the posterior portion of the medial surface of the brain. PMC comprises several distinct regions, including posterior cingulate cortex (PCC), retrosplenial cortex (RSC), and the precuneus, among others (Cauda et al. 2010; Bzdok et al. 2015). Scientific interest in PMC has largely stemmed from a seminal neuroimaging study showing that the region is highly active in healthy adults at rest (Raichle et al. 2001). This study demonstrated that PCC and the adjacent precuneus have blood flow and glucose consumption levels elevated about 40% above the whole-brain average, suggesting that these regions are highly important for cortical information processing. Studies have further shown that this resting state activity in PMC intrinsically correlates with that in several other areas of cortex, forming a so-called default mode network (DMN) (Raichle et al. 2001; Leech et al. 2011; Greicius et al. 2009; Buckner et al. 2008). There is no consensus regarding the specific functions of PMC, however, which likely explains its absence from many systems-level models of brain function.

The existing literature implicates PMC subregions in several different functions and disorders. For example, PCC exhibits increased activity during cognitive tasks involving semantic processes, episodic memory retrieval, autobiographical memory, and planning (Addis et al. 2007; Mason et al. 2007; Huijbers et al. 2012; Krieger-Redwood et al. 2016; Vatansever et al. 2017a). Furthermore, it features early amyloid deposition and reduced metabolism in Alzheimer's disease (Sperling et al. 2009; Greicius et al. 2004; Buckner et al. 2008). The precuneus is related to visuospatial imagery, episodic memory retrieval, self-processing, and consciousness (Cavanna and Trimble 2006). In addition, the precuneus is associated with visually guided reaching impairment termed 'optic ataxia' via underlying parietal white matter (Karnath and Perenin 2005). Finally, RSC has been associated with episodic memory, spatial navigation, imagination, and planning (Vann et al. 2009). Moreover, RSC has been linked to memory impairment and spatial disorientation (Rudge and Warrington 1991; Maguire 2001; Osawa et al. 2006). While each of these regions has distinct functions, there is

✉ Sven Vanneste
sven.vanneste@utdallas.edu
http://www.lab-clint.org

[1] Lab for Clinical and Integrative Neuroscience, School of Behavioral and Brain Science, University of Texas at Dallas, 800 W Campbell Rd, Richardson, TX 75080, USA

[2] Department of Surgical Sciences, Dunedin School of Medicine, University of Otago, Dunedin, New Zealand

clearly also a significant degree of overlap, e.g., episodic memory.

Although there is a substantial body of literature investigating PMC function, there has been minimal effort to disentangle the functions of its subregions in an unbiased way. To date, meta-analyses of different brain regions have either (1) defined a specific subset of cognitive functions as a priori important to the regions of interest (Shackman et al. 2011) and/or (2) focused only on a specific region of interest (Palomero-Gallagher et al. 2015). Our present study addresses these issues by conducting an unbiased meta-analysis of PMC function using Neurosynth (http://neurosynth.org), a database featuring 11,406 studies from the fMRI literature (Yarkoni et al. 2011). We replicate a method previously used to map medial and lateral frontal cortex (de la Vega et al. 2016, 2017), applying it here to PMC. The specific aim of this meta-analysis is to create a comprehensive and data-driven map of PMC subregions based on a broad profile of functions and disorders.

Methods

The following methods were replicated from previous studies by Alejandro de la Vega and colleagues (de la Vega et al. 2016, 2017; Dixon et al. 2018), using the Python code and data available freely online at https://github.com/adelavega/neurosynth-mfc and https://github.com/adelavega/neurosynth-lfc. We apply the techniques used in those studies to PMC here, rather than to medial or lateral frontal cortex; see Fig. 1 for a visual summary.

Dataset

The dataset we used in this project is Version 0.6 of the Neurosynth database (Yarkoni et al. 2011) which contains 413,428 activation peaks from 11,406 fMRI studies. Besides these peaks, Neurosynth also contains all the words from the abstracts of every included study, from which a previous study generated 60 different topics (de la Vega et al. 2016). All activation peaks and subsequent analyses are in the MNI-152 coordinate space (Mazziotta et al. 1995).

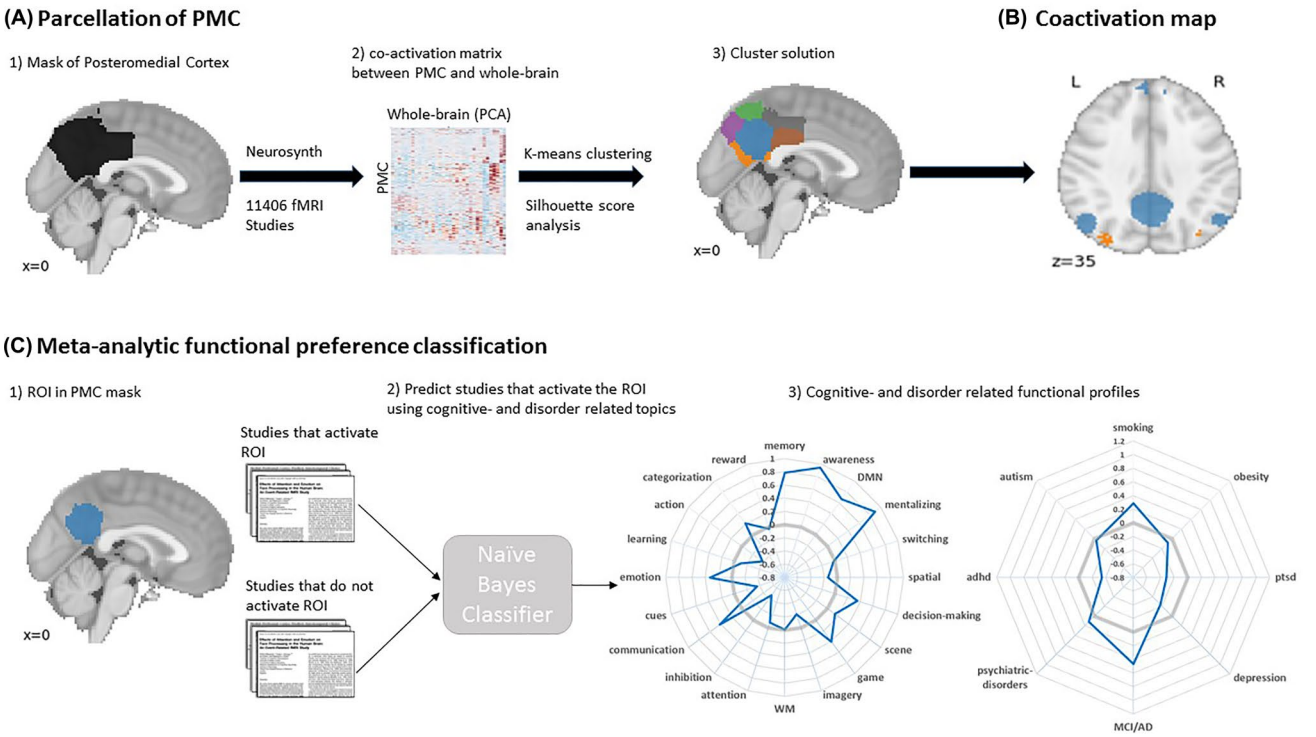

Fig. 1 Graphical summary of the methods used in the present study. **a** We parcellated our PMC mask based on whole-brain coactivation patterns retrieved from the Neurosynth database. Parcellation was done based on *k*-means clustering, taking the solution that performed the best on a silhouette score analysis (i.e., $k=6$). **b** We then generated coactivation maps from each of these clusters for comparison. **c** We used a meta-analytic functional preference classification to determine which among 20 cognitive function-related topics and 8 disorder-related topics can best predict the activity within each cluster. *PMC* posteromedial cortex

PMC mask

In previous studies (de la Vega et al. 2016, 2017), the authors used the Harvard–Oxford (H–O) anatomical atlas and H–O probabilistic atlas to create their masks of frontal cortex (Desikan et al. 2006). We do the same here to create our PMC mask. To cluster the voxels inside the PMC area from the whole-brain clustering matrix, we generated a binarized PMC mask. First, we used the FMRIB Software Library (FSL) to combine the PCC—which already included the RSC—and the precuneus from the H–O anatomical atlas (http://www.fmrib.ox.ac.uk/fsl/) to generate a PMC anatomical mask. Then, we excluded voxels with less than 30% probability of falling into cortical gray matter by masking the H–O probabilistic atlas ($P > 30\%$) using the PMC anatomical mask and binarized it (Fig. 1a.1).

Coactivation clustering

We applied a method used in previous studies (de la Vega et al. 2016, 2017) to analyze the voxels inside the PMC mask by calculating the coactivation matrix between the PMC voxels and those in the rest of the brain (including subcortical areas) based on their coactivation pattern from the Neurosynth database. We represented coactivation in each voxel as a binary vector of length 11,406 (the number of studies); a value of 1 means that the voxel falls within 10 mm of the activation coordinate reported in a particular study, and a value of 0 means the opposite. For the clustering, we also excluded voxels with low activation rates (i.e., with fewer than 100 studies reporting activation of that voxel).

Before calculating the coactivation matrix, we performed a principal component analysis (PCA) on the whole brain to reduce its total variance down to 100 components. This reduces the size of the coactivation matrix from [9365 × 151,527] (PMC voxels × whole-brain voxels) to [9365 × 100] (PMC voxels × principal components), which makes clustering computationally feasible (Fig. 1a.2). We used a *k*-means clustering algorithm from scikit-learn Python package (Pedregosa et al. 2011) to group the PMC voxels into 2–20 clusters. We also calculated the Pearson correlation distance between every voxel in the PMC mask and each principal component so that we could perform a silhouette score analysis on the coactivation matrix to select the ideal number of clusters (Fig. 1a.3).

Silhouette score analysis

As noted in de la Vega et al. (2017), an unstandardized coactivation matrix will result in relatively unevenly sized clusters. This is because voxels with higher activation rates tend to form smaller clusters, even though there are no significant functional differences between these voxels. By standardizing the coactivation matrix, we can ensure that the clustering procedure is driven by the relative differences in whole-brain coactivation rather than relative differences in overall activation rate. It is impossible to determine the "correct" number of clusters in any abstract sense, since that number depends heavily on researchers' goals, methods of analysis, and data quality (de la Vega et al. 2016, 2017; Eickhoff et al. 2015). However, silhouette score analysis offers a valid and objective method to determine the optimal number of clusters for our present study by calculating the within-cluster cohesion of the voxels in our PMC mask (de la Vega et al. 2016, 2017). The silhouette score is calculated using $(b - a)/\max(a, b)$, where a is the mean intra-cluster distance for each voxel and b is the mean nearest-cluster distance for each voxel. Greater silhouette scores correspond with smaller mean within-cluster distances, which in turn means better within-cluster cohesion.

Coactivation profiles

After determining the optimal number of clusters, we compared the whole-cortex coactivation pattern of each PMC cluster to the adjacent cluster (de la Vega et al. 2016, 2017) to map out the differences in coactivation patterns. To do this, we used a meta-analytic approach to contrast studies that activated a given cluster to studies that activated the adjacent cluster. The resulting image reveals voxels across all of cortex that shows greater probability of coactivating with the given cluster than the average of adjacent clusters. We conducted a two-way Chi square test between two sets of studies and applied a threshold to the coactivation images using the false discovery rate (FDR) correction for multiple comparisons such that the included voxels are significant at the $p_{FDR} < 0.01$ level (Fig. 1b).

Meta-analytic functional preference profiles

To map out different functional preference profiles related to different PMC clusters, by using the same dataset with 60 identical topics. To resolve the redundancy and ambiguity issues caused by term-based analysis, the previous paper (de la Vega et al. 2016) derived a set of 60 topics using latent Dirichlet allocation topic modeling (David et al. 2003). By excluding 25 topics that are unrelated to psychological phenomena and based on the mean log odds ratio (LOR) scores, we picked out 20 functional topics for $k = 6$ cluster (Table 1). Furthermore, we included all eight disorder topics for $k = 6$ cluster for the following meta-analytic procedure (Table 2).

For the purposes of generating functional preference profiles that best predict each cluster, we first selected two different sets of studies: (1) studies that at least activated 5% of voxels within a given cluster and (2) studies that activated no voxels within a given cluster. We then trained a naïve

Table 1 Functional topics most strongly associated with PMC regions

Topic	Top words
Memory	Memory, retrieval, encoding, recognition, episodic, items, recall, words, memories, recollection
Awareness	Awareness, future, conscious, default, consciousness, past, rate, heart, mental, personal
DMN	Default, intrinsic, seed, spontaneous, thickness, developmental, adolescence, values, childhood, global
Mentalizing	Social, empathy, moral, person, judgments, mentalizing, mental, mind, judgment, perspective
Switching	Switching, rule, executive, switch, rules, flexibility, shifting, aggression, shift, aggressive
Spatial	Spatial, adaptation, location, space, rotation, mental, orientation, position, visuospatial, navigation
Decision-making	Decision, choice, decisions, choices, risk, reward, outcome, outcomes, uncertainty, risky
Scene	Scenes, scene, complexity, effort, demands, visual, manipulation, easy, difficult, natural
Game	Acupuncture, game, unfair, stimulation, offers, playing, acupoint, cooperation, social, provocation
Imagery	Imagery, mental, imagined, motor, gait, walking, generation, imagination, locomotion, imagine
WM	Memory, working, WM, load, verbal, maintenance, delay, encoding, capacity, executive
Attention	Attention, attentional, visual, spatial, search, location, orienting, target, attended, irrelevant
Inhibition	Inhibition, inhibitory, stop, motor, sustained, no-go, transient, suppression, inhibit, inhibited
Communication	Gestures, BPD, gesture, communication, communicative, speech, actor, chemotherapy, iconic, nonverbal
Cues	Cues, cue, target, reaction, preparation, anticipation, RT, cued, visual, times
Emotion	Emotional, emotion, regulation, affective, pictures, emotions, arousal, affect, reappraisal, viewing
Learning	Learning, feedback, learned, sequence, implicit, training, explicit, reinforcement, associative, transfer
Categorization	Category, reasoning, categories, categorization, relations, similarity, categorical, relational, abstract, perceptual
Action	Action, actions, motor, goal, mirror, planning, imitation, execution, directed, movements
Reward	Reward, sleep, anticipation, monetary, rewards, motivation, incentive, loss, motivational, gain

Strongest loading words for each topic are listed in descending order of association strength

DMN default mode network, *WM* working memory, *BPD* borderline personality disorder, *RT* reaction time

Table 2 Disorder topics and their top-loading words

Topic	Top words
PTSD	PTSD, blind, sighted, trauma, traumatic, TBI, stress, experts, survivors, novices
ADHD	ADHD, users, cocaine, drug, cannabis, hyperactivity, attention, deficit, addiction, CD
Depression	Depression, MDD, depressive, bipolar, depressed, anxiety, mood, major, BD, sad
Autism	Autism, grey, aging, lesion, compensatory, executive, deficit, abilities, intelligence, tests
Obesity	Food, weight, eating, obese, women, foods, obesity, nervosa, energy, caloric
Psychiatric-disorders	Schizophrenia, psychosis, hallucinations, psychotic, SZ, schizophrenic, episode, impairments, illness, verbal
Smoking	ASD, stress, smokers, smoking, epilepsy, nicotine, cortisol, craving, heroin, drug
MCI/AD	AD, PD, Alzheimer, mild, aMCI, Parkinson, dementia, loss, stage, human

Strongest loading words for each topic are listed in descending order of association strength

PTSD posttraumatic stress disorder, *ADHD* attention deficit disorder, *MCI* mild cognitive impairment, *AD* Alzheimer's disease, *TBI* traumatic brain injury, *CD* conduct disorder, *MDD* major depressive disorder, *BD* bipolar disorder, *SZ* schizophrenia, *ASD* acute stress disorder, *PD* Parkinson's disease, *aMCI* amnestic mild cognitive impairment

Bayesian classifier to discriminate these two sets of studies based on the loading of cognitive function and disorder-related topics onto individual studies for each cluster. The resulting model predicts the probability that an fMRI study activated a cluster, given the sematic content of that study (Fig. 1c).

We extracted the log odds ratio (LOR) of each topic from the naïve Bayesian model to create functional preference profiles for each cluster. The LOR is defined here as the ratio between the probability of a given topic in the set of active studies and in the set of inactive studies. A positive LOR for a given topic means that the topic is predictive for the activation of the given cluster. We then determine the statistical significance of the LOR using permutation testing. To do this, we permuted the class labels, extracted the LOR for each topic 1000 times, and obtained a null distribution of LORs for each topic and each cluster. We calculated the *p* values for each pairwise relationship between topics and

clusters and reported significance at the 0.01 level for the 20 cognitive function-related topics and 0.05 level for the eight disorder-related topics, including the FDR correction for multiple comparisons.

Finally, we determined whether certain topics show a preference for a particular cluster. We conducted exploratory, post hoc comparisons by examining if the 95% confidence interval (CI) for the LOR of a specific topic for a given cluster overlaps with the 95% CIs of the same topic in other clusters. To do this, we applied the procedure used in de la Vega et al. (2016, 2017), i.e., using bootstrapping by sampling with replacement and recalculating LOR for each cluster 1000 times. As the comparisons are post hoc and exploratory, caution is warranted in interpreting their results.

Functional lateralization analysis

We also tested for differences between left and right PMC. To this end, we first split the PMC mask into left- and right-hemispheric masks. We then replicated the same silhouette score analysis, coactivation clustering, coactivation profiles, and meta-analytic functional preference profiles analysis on both the left and right PMC masks.

Results

Functionally separable regions in PMC

Based on the silhouette score analysis (Fig. 2a), PMC was subdivided into six bilateral clusters along the midline axis (Fig. 2b). To contextualize these clusters in terms of anatomy, we compared them to the H–O probabilistic structural atlas. We did not expect that these functionally defined clusters would be precisely constrained by the H–O atlas' anatomical boundaries, but we did nevertheless observe a moderate correspondence. This finding reflects the notion that functional areas are not necessarily the same as anatomical areas, but that functions should nevertheless have some anatomical basis.

In the anterior part of PMC, we identified two clusters that correspond to superior dorsal PCC (sdPCC) and inferior dorsal PCC (idPCC), which is similar to the anatomical parcellation reported in a previous review paper (Leech and Sharp 2014). However, the sdPCC extended superiorly into the anterior precuneus and both sdPCC and idPCC extended to pMCC (Fig. 2b). This is because the H–O atlas we used to generate our PMC mask divided the cingulate only into the anterior and posterior portions.

In the dorsal posterior part of the PMC, we identified two clusters that correspond to the anatomical location of the precuneus, which we labeled as anterior precuneus (aPrC) and posterior precuneus (pPrC) (Fig. 2b). A previous review

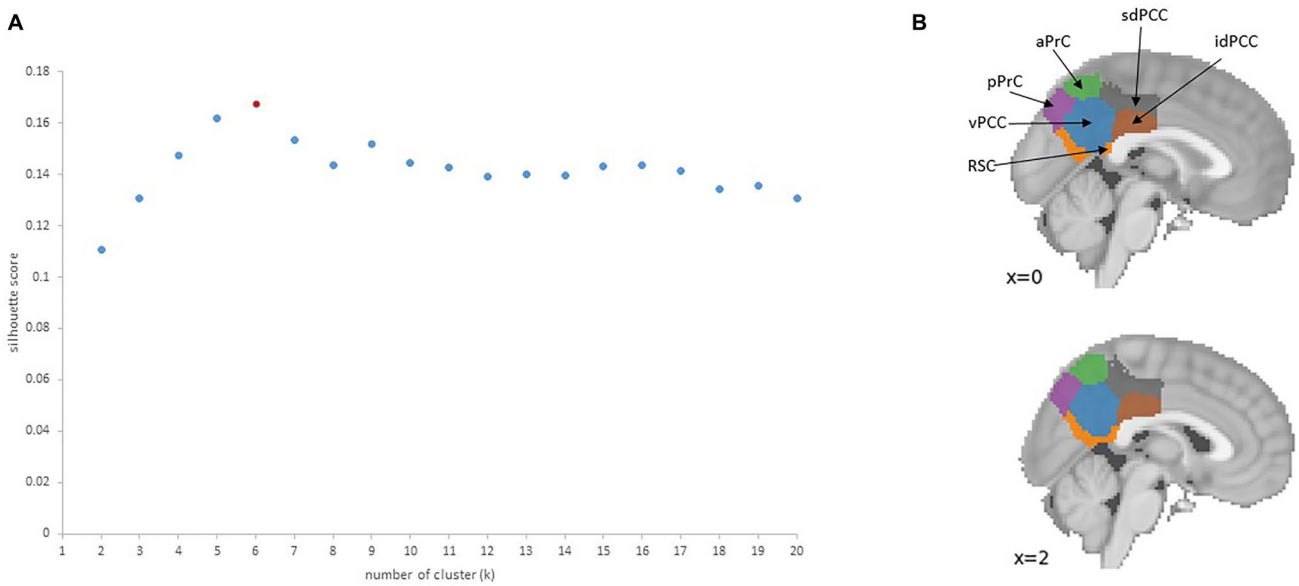

Fig. 2 Coactivation-based clustering of PMC results. **a** The silhouette scores, a measure for intra-cluster cohesion, for clusters from $k=2$ to $k=20$ (p values for all clusters <0.001). Red dots represent the cluster solution we picked out for this study. **b** Sagittal views of the $k=6$ solution ($x=0$ and 2). *RSC* retrosplenial cortex, *vPCC* ventral posterior cingulate cortex, *pPrC* posterior precuneus, *aPrC* anterior precuneus, *sdPCC* superior dorsal posterior cingulate cortex, *idPCC* inferior dorsal posterior cingulate cortex

paper (Cavanna and Trimble 2006) did provide some preliminary evidence for subdividing the precuneus into the anterior and posterior regions in this way based on activation patterns.

In the ventral part of PMC, we identified two clusters representing the ventral PCC (vPCC) and retrosplenial cortex (RSC) (Fig. 2b). Note that our vPCC cluster extended partially into the ventral precuneus and dPCC. Leech and Sharp (2014) subdivided the vPCC into superior and inferior vPCC. Our six-cluster solution, however, represented these two Brodmann regions (v31 and v23) with a single cluster (vPCC). This suggests that two adjacent regions can express similar functional profiles despite having distinct cytoarchitectural characteristics. Our second cluster, which we identified as RSC, extended dorsally and posteriorly into the ventral part of the precuneus and PCC.

Meta-analytic coactivation and functional preference profiles

Anterior PMC

We contrasted the coactivation patterns between the sdPCC and idPCC (Fig. 3a) to identify voxels with higher coactivation degree with one cluster than the other. Our result showed that the coactivation patterns of these two clusters are similar, except that idPCC showed greater coactivation with bilateral anterior insula than sdPCC (Fig. 3b).

Of the cognitive function-related topics, permutation significance testing showed both that idPCC and sdPCC are significantly associated with 'memory' and 'decision-making' and that idPCC is significantly associated with 'reward' (Fig. 3c). However, exploratory post hoc tests did not show a significant difference between idPCC and sdPCC in association with 'reward' (95% CI LOR: reward: idPCC [0.12, 0.59], sdPCC [− 0.27, 0.3]) (Fig. 6a). Of the disorder-related topics, idPCC is significantly associated with 'smoking' (Fig. 3d). However, exploratory post hoc tests did not show a significant difference between idPCC and sdPCC in this topic also (95% CI LOR: smoking: idPCC [− 0.05, 0.55], sdPCC [− 0.47, 0.26]) (Fig. 6b).

Dorsal PMC

We similarly contrasted the coactivation patterns between aPrC and pPrC (Fig. 4a). We found that the coactivation patterns of these two clusters are also similar, except that pPrC showed greater coactivation with idPCC than aPrC (Fig. 4b).

Of the cognitive function-related topics, permutation significance testing showed that activity in both pPrC and aPrC is significantly predicted by 'working memory' (WM) and 'spatial' (Fig. 4c). We also found that pPrC is significantly associated with 'memory', 'cues', and 'decision-making' while aPrC is significantly associated with 'imagery' (Fig. 4c). However, we only found pPrC to be more strongly associated with 'memory' than aPrC in the exploratory post hoc tests (95% CI LOR: memory: pPrC [0.67, 0.97], aPrC [− 0.06, 0.3]) (Fig. 6a). Of the disorder-related topics, a permutation test suggested that no topics were significantly associated with activity in either aPrC or pPrC (Fig. 4d).

Ventral PMC

Lastly, we contrasted the coactivation patterns between the vPCC and RSC (Fig. 5a). We found that the vPCC coactivated more with bilateral temporal parietal junction (TPJ), temporal cortex, and ventral medial prefrontal cortex (vmPFC), whereas the RSC coactivated more with parahippocampal/hippocampal cortex (Fig. 5b).

Of the cognitive function-related topics, permutation significance tests showed that activity in both vPCC and RSC is significantly associated with 'memory', 'awareness', and 'decision-making' (Fig. 5c). We also found that vPCC has significant associations with 'DMN', 'mentalizing', 'emotion', and 'communication', while RSC has significant associations with 'spatial', 'scene', and 'imagery' (Fig. 5c). The exploratory post hoc tests suggested that vPCC was more strongly associated with 'mentalizing' (95% CI LOR: mentalizing: vPCC [0.75, 1.02], RSC [− 0.04, 0.35]) and RSC was more strongly associated with 'spatial' and 'imagery' (95% CI LOR: spatial: vPCC [− 0.4, 0.06], RSC [0.25, 0.8]; imagery: vPCC [− 0.5, 0.07], RSC [0.16, 0.82]) (Fig. 6a). Of the disorder-related topics, permutation significance tests showed that vPCC was significantly predicted by 'smoking' and 'MCI/AD' (Fig. 5d).

Functional lateralization analysis

After we split the PMC mask into the left and right halves and replicated the same analyses on both halves, we obtained six-cluster parcellations and functional preference profiles for both left and right PMC, analogous to that of our whole PMC mask from earlier. For this reason, the clusters in the left/right masks followed the same naming scheme as the clusters in the whole PMC mask. However, as indicated by the permutation significance tests, there were some differences between the correlation of functional preference profiles with left and right PMC.

Of the cognitive function-related topics, left pPrC was significantly associated with 'spatial', while right pPrC was significantly associated with 'cues'. Left aPrC was also significantly associated with 'imagery', while the right aPrC was not. The left idPCC was significantly associated with 'awareness', while the right idPCC was not. The left vPCC was significantly associated with 'emotion' and 'communication', while the right vPCC

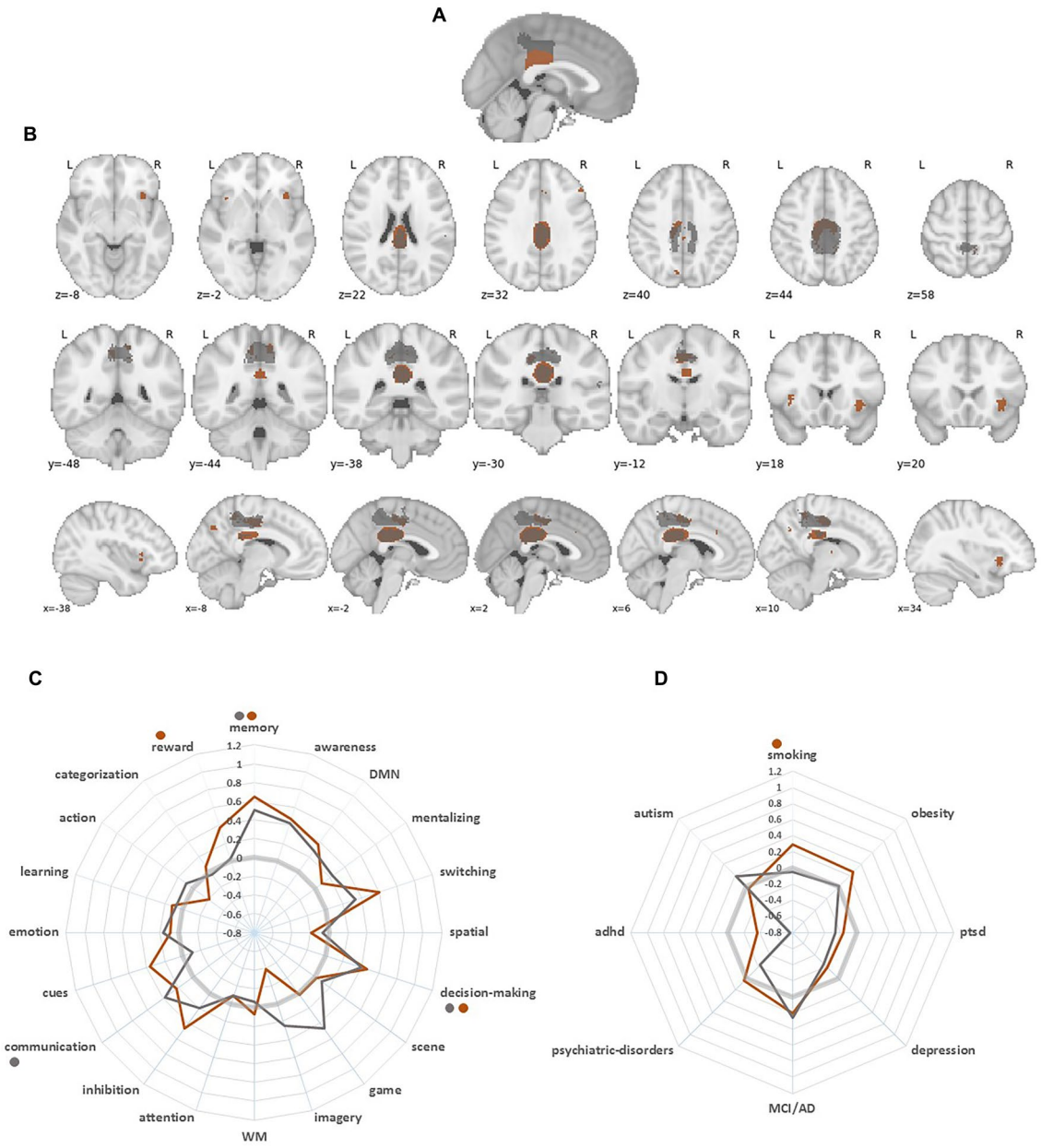

Fig. 3 Detailed results for the sdPCC (gray) and idPCC (brown) clusters obtained using the $k=6$ solution, a.k.a. anterior PMC. **a** Midsagittal view of the two selected clusters. **b** Coactivation comparison of the two selected clusters presented using axial, coronal, and sagittal slice views. **c** Functional preference profiles of the two selected clusters using 20 functional topics. **d** Functional preference profiles of the two selected clusters using eight disorder-related topics. For both **c, d**, functional preference is measured using the LOR. Significance was determined using permutation testing and indicated on the radar plots as color-coded dots. The significance thresholds for **c, d** were 0.01 and 0.05, respectively, including the FDR correction for multiple comparisons. *sdPCC* superior dorsal posterior cingulate cortex, *idPCC* inferior dorsal posterior cingulate cortex, *PMC* posteromedial cortex, *LOR*, log odds ratio, *FDR* false discovery rate

was not. The left RSC was significantly associated with 'decision-making' and 'imagery', while the right RSC was significantly associated with 'spatial' (Fig. 7). Of the disorder-related topics, the left vPCC was significantly associated with 'smoking', while the right RSC was significantly associated with 'MCI/AD' (Fig. 8). However, the exploratory post hoc tests for cognitive function- and disorder-related topics in both the left and right PMC did not show any significant differences in the functional profiles mentioned above (Figs. 9, 10).

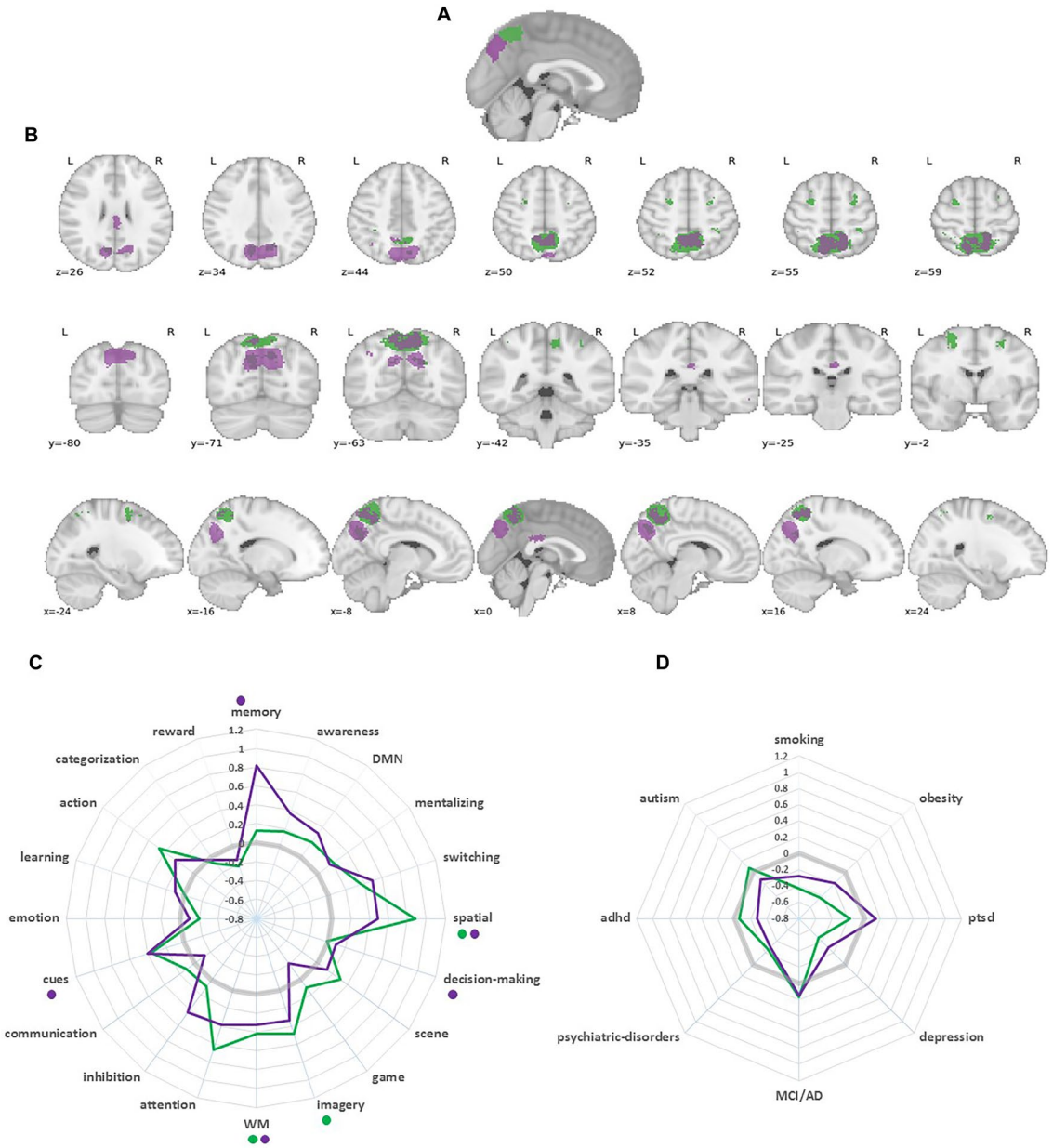

Fig. 4 Detailed results for the aPrC (green) and pPrC (purple) clusters obtained using the $k=6$ solution, a.k.a. dorsal PMC. **a** Mid-sagittal view of the two selected clusters. **b** Coactivation comparison of the two selected clusters presented using axial, coronal, and sagittal slice views. **c** Functional preference profiles of the two selected clusters using 20 functional topics. **d** Functional preference profiles of the two selected clusters using eight disorder-related topics. For both **c, d**, functional preference is measured using the LOR. Significance was determined using permutation testing and indicated on the radar plots as color-coded dots. The significance thresholds for **c, d** were 0.01 and 0.05, respectively, including the FDR correction for multiple comparisons. *aPrC* anterior precuneus, *pPrC* posterior precuneus, *PMC* posteromedial cortex, *LOR* log odds ratio, *FDR* false discovery rate

Discussion

We identified six clusters that roughly separate PMC into anterior (sdPCC and idPCC), dorsal (aPrC and pPrC), and ventral (vPCC and RSC) divisions. Based on the exploratory nature of our present study, the boundaries between different clusters that characterize anatomical regions should not be taken literally. However, this functional parcellation map provides a snapshot of different subregions within PMC. Our results support the idea that subregions in PMC have some shared functions such as 'memory' and 'decision-making'. This is in line with previous studies suggesting that areas in DMN, specifically PMC, make major contributions to memory-related processes

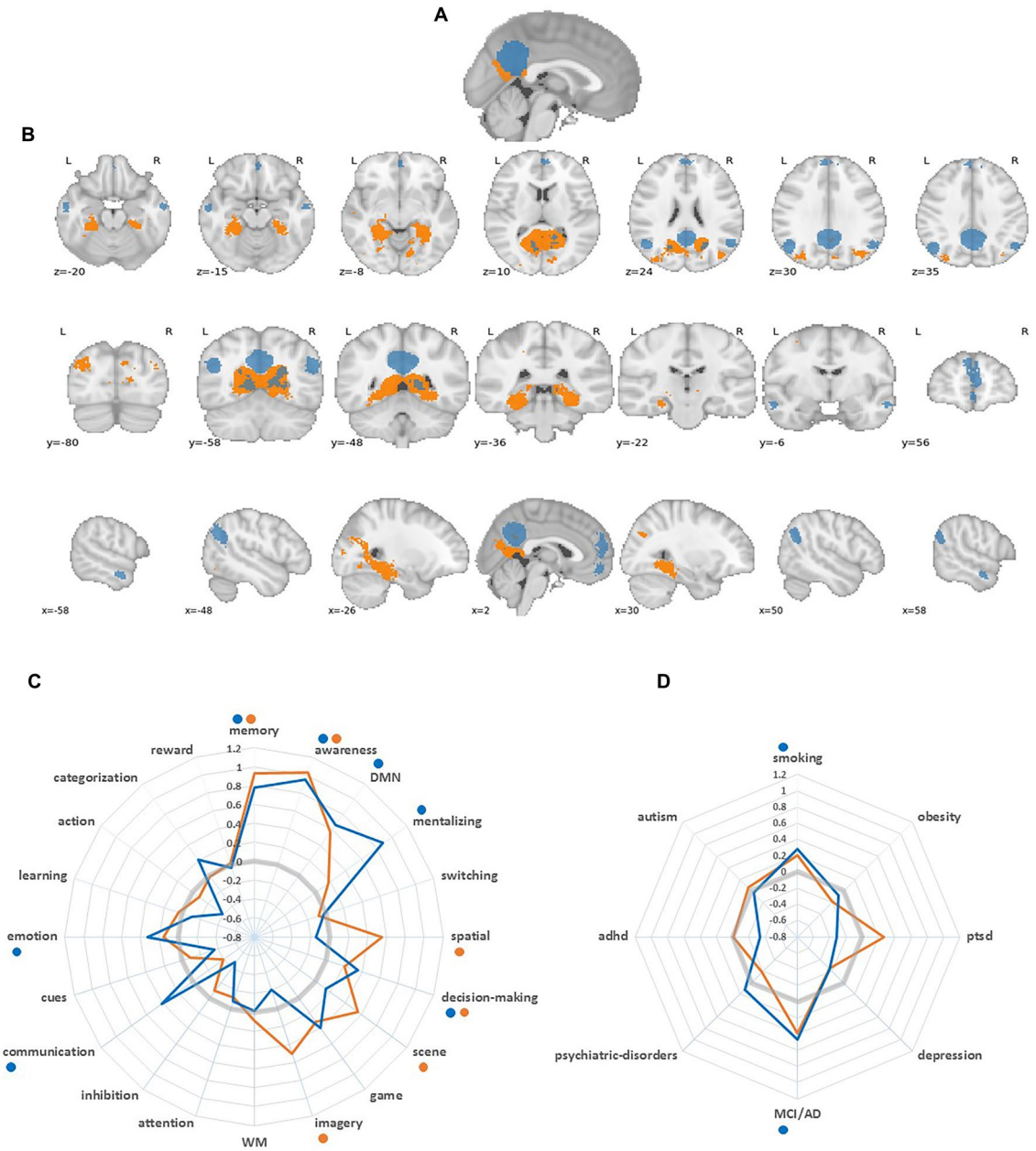

Fig. 5 Detailed results for the vPCC (blue) and RSC (orange) clusters obtained using the $k=6$ solution, a.k.a. ventral PMC. **a** Mid-sagittal view of the two selected clusters. **b** Coactivation comparison of the two selected clusters presented using axial, coronal, and sagittal slice views. **c** Functional preference profiles of the two selected clusters using 20 functional topics. **d** Functional preference profiles of the two selected clusters using eight disorder-related topics. For both **c, d**, functional preference is measured using the LOR. Significance was determined using permutation testing and indicated on the radar plots as color-coded dots. The significance thresholds for **c, d** were 0.01 and 0.05, respectively, including the FDR correction for multiple comparisons. *vPCC* ventral posterior cingulate cortex, *RSC* retrosplenial cortex, *PMC* posteromedial cortex, *LOR* log odds ratio, *FDR* false discovery rate

and automated information processing to make fast and efficient decisions (Margulies et al. 2016; Margulies and Smallwood 2017; Vatansever et al. 2017c). At the same time, given clusters or combinations of clusters are also functionally distinct. Examples include: aPrC and pPrC, which were both associated with 'WM';idPCC and showed associations with 'reward' and 'smoking'; and vPCC, which showed associations with 'DMN', 'mentalizing', and 'MCI/AD'. We discuss our findings (summarized in Fig. 11) in detail below and place them in the context of the literature.

Fig. 6 Strength of association, measured using LOR between the six clusters and the topics of interest: **a** cognitive function-related topics; **b** disorder-related topics. For each association, we generated 95% CIs using a bootstrapping test that resampled 1000 times. *LOR* log odds ratio, *CI* confidence interval

Functional preference profiles within PMC

Anterior PMC

In the anterior part of PMC, our analysis identified two clusters, which we defined as sdPCC and idPCC. This regional separation based on functional aspects results in a similar organization to the actual anatomical location of dorsal PCC (Vogt 2009). Both sdPCC and idPCC are associated with 'memory' and 'decision-making'. This was somewhat surprising because a primate structural connectivity study found that the connection between the hippocampal formation, parahippocampal cortex, and dorsal PCC was less prominent compared to vPCC and RSC (Kobayashi and Amaral 2007). However, the idPCC showed associations with 'reward' and 'smoking'. Primate structural connection

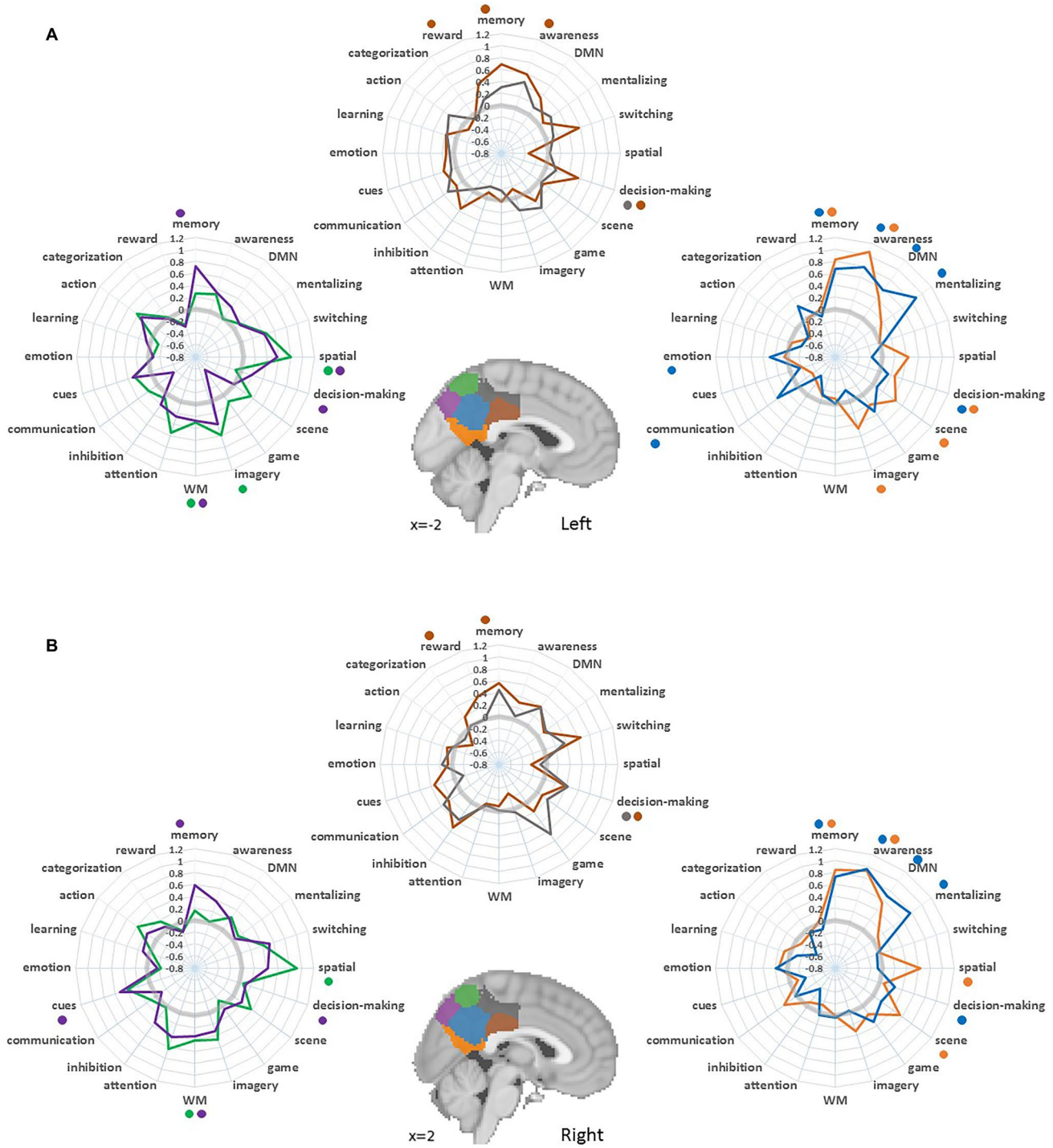

Fig. 7 Lateralization analysis of $k=6$ cluster solutions generated separately for **a** left and **b** right PMC masks. Sagittal slice views at $x = -2$ and 2, respectively, display the clusters themselves. Radar plots display the functional preferences profiles across 20 cognitive function-related topics for each cluster using LOR. Dots indicate permutation-based significance at the 0.01 level, including the FDR correction for multiple comparisons. *PMC* posteromedial cortex, *LOR* log odds ratio, *FDR* false discovery rate

and alcohol-related craving studies have revealed that PCC had dense structural connections as well as functional correlations with regions that are important to the reward system such as dACC, thalamus, insula, and striatum (Parvizi et al. 2006; Huang et al. 2018; Romanski et al. 1997; Yeterian and Pandya 1988; Kunishio and Haber 1994; Vogt et al. 1987). Combining these associated topics, anterior PMC might play an important role in the formation of habitual behavior

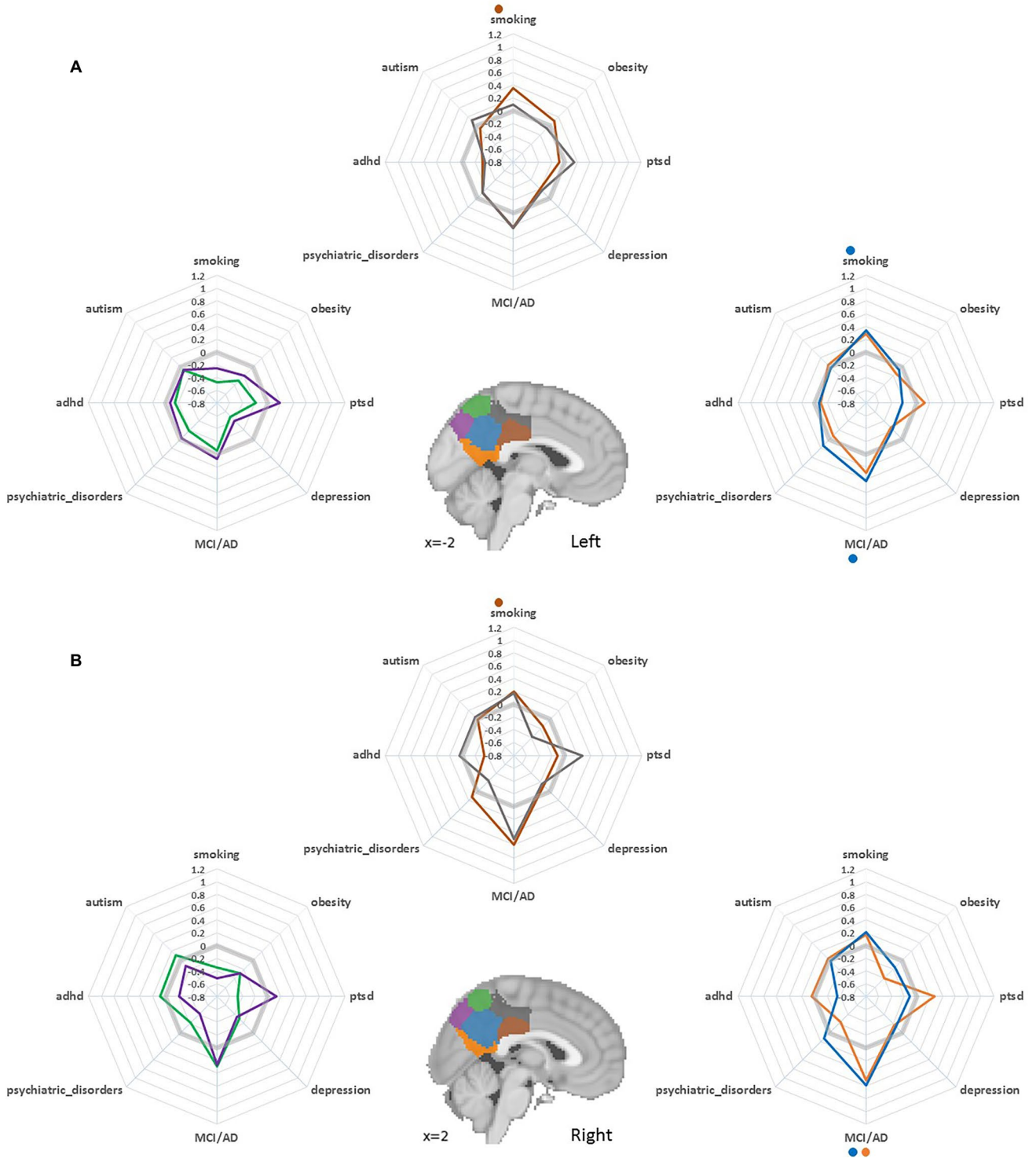

Fig. 8 Lateralization analysis of $k=6$ cluster solutions generated separately for the **a** left and **b** right PMC masks. Sagittal slice views at $x = -2$ and 2, respectively, display the clusters themselves. Radar plots display the functional preferences profiles across eight disorder-related topics for each cluster using LOR. Dots indicate permutation-based significance at the 0.05 level, including the FDR correction for multiple comparisons. *PMC* posteromedial cortex, *LOR* log odds ratio, *FDR* false discovery rate

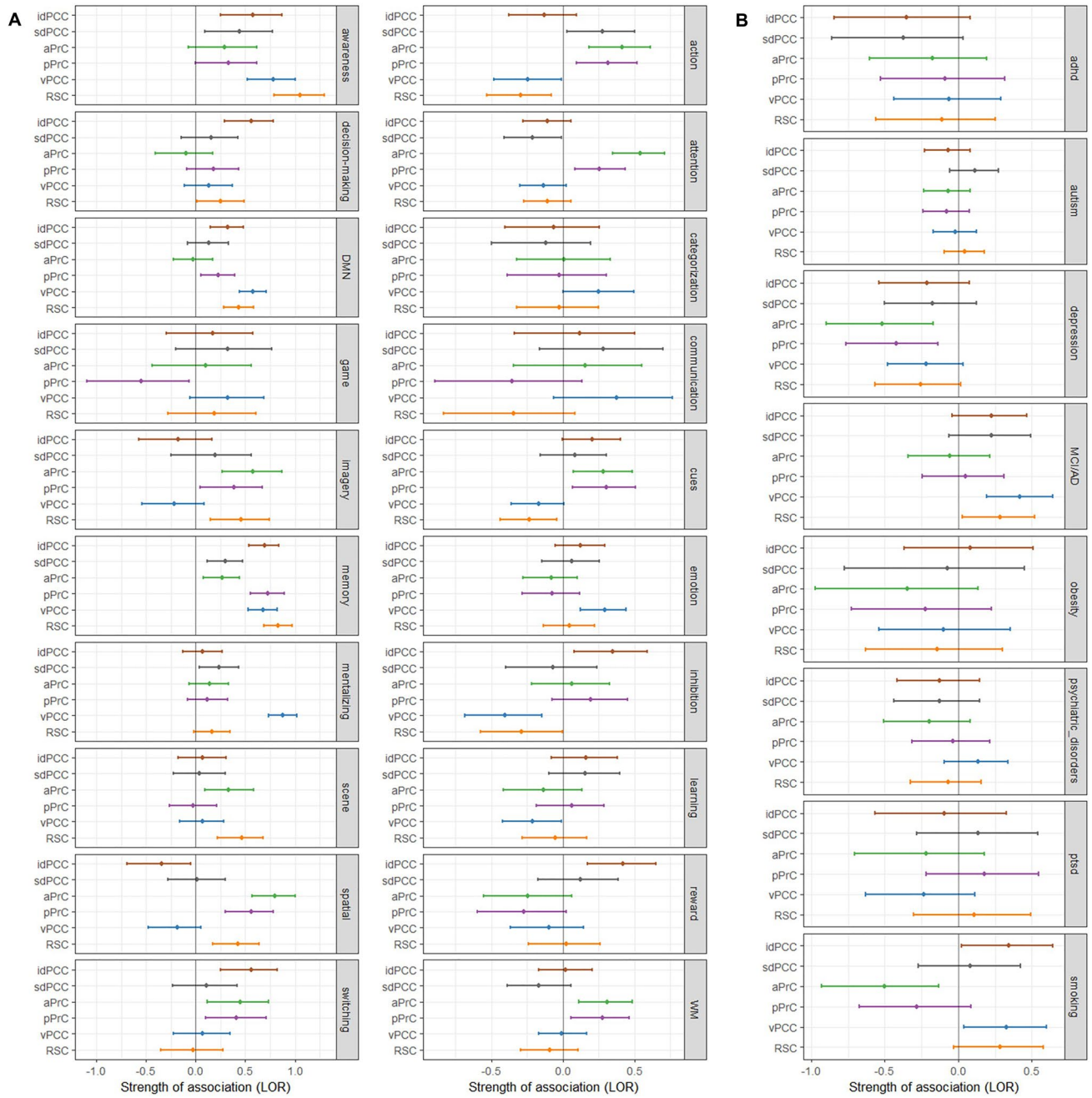

Fig. 9 Strength of association, measured using LOR, between the six clusters from the left PMC mask and the topics of interest: **a** cognitive function-related topics; **b** disorder-related topics. For each association, we generated 95% CIs using a bootstrapping test that resampled 1000 times. *LOR* log odds ratio, *PMC* posteromedial cortex, *CI* confidence interval

through decision-making and cognitive flexibility (Vatansever et al. 2016, 2017c).

Dorsal PMC

In the dorsal part of PMC, our analysis identified two clusters, which we defined as aPrC and pPrC. In the functional preference analysis, the activity of both regions was predicted by 'working memory' (WM) and 'spatial'. This is in line with the majority of previous findings, supporting the central role of the precuneus in visuospatial information processing (Cavanna and Trimble 2006) as well as working memory (Fransson 2006; Hampson et al. 2010; Vatansever et al. 2015, 2017b). Furthermore, the application of transcranial magnetic stimulation (TMS) to a midline parietal site centered on the precuneus resulted in the facilitation

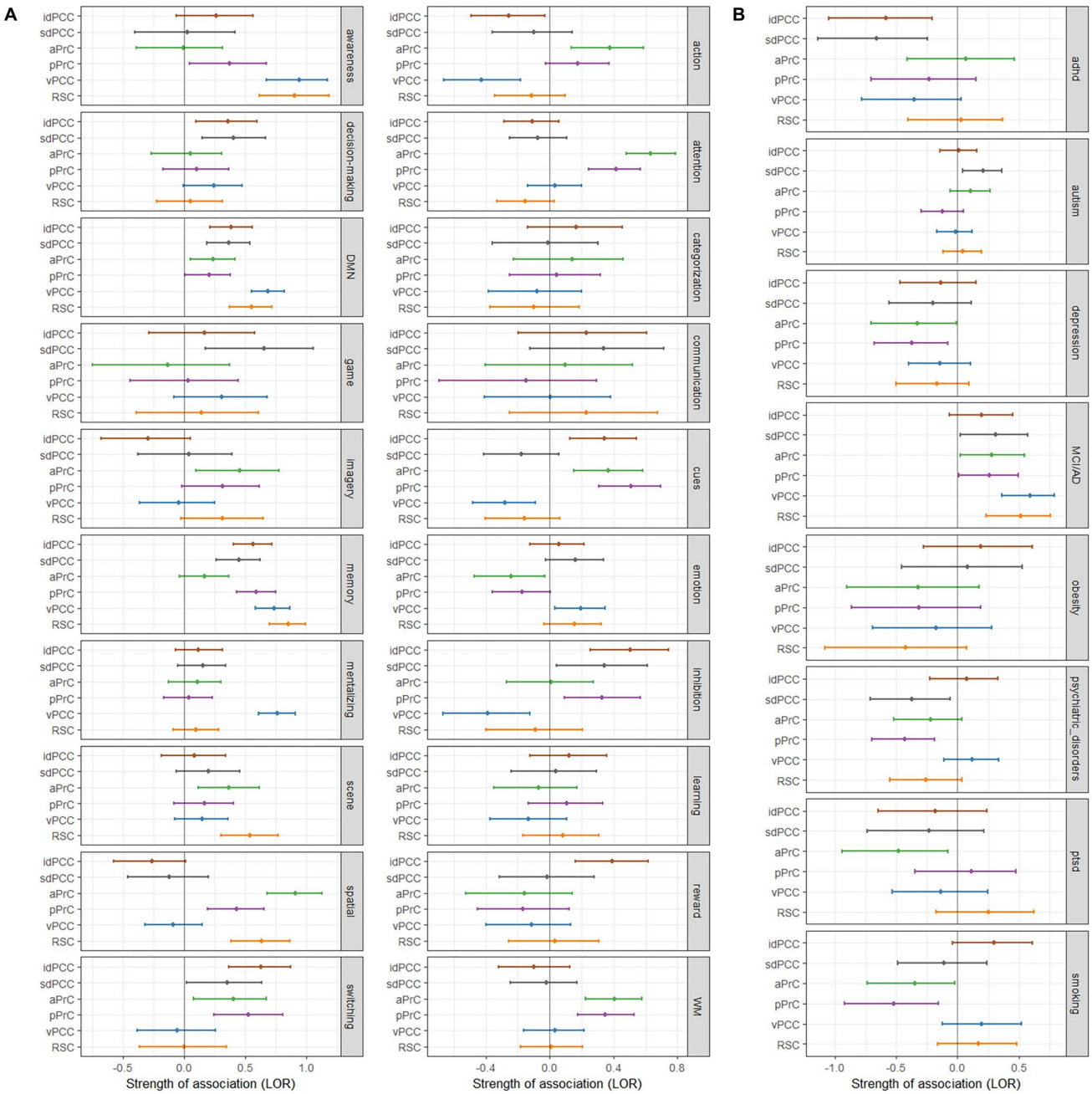

Fig. 10 Strength of association, measured using LOR, between the six clusters from the right PMC mask and the topics of interest: **a** cognitive function-related topics; **b** disorder-related topics. For each association, we generated 95% CIs using a bootstrapping test that resampled 1000 times. *LOR* log odds ratio, *PMC* posteromedial cortex; *CI* confidence interval

of performance in a delayed-match-to-sample (DMS) task (Luber et al. 2007). The pPrC is significantly associated with 'memory', while the aPrC is significantly associated with 'imagery'. This result is consistent with the idea that the precuneus can be subdivided into an anterior region involved in self-centered mental imagery and a posterior region subserving successful episodic memory retrieval (Cavanna and Trimble 2006).

Ventral PMC

In the ventral part of PMC, our analysis identified two clusters, which we defined as vPCC and RSC. These two clusters were both highly predicted by 'memory', 'awareness', and 'decision-making'. As previously mentioned, vPCC and RSC have dense connections to the medial temporal lobe, hippocampal formation, and parahippocampal cortex

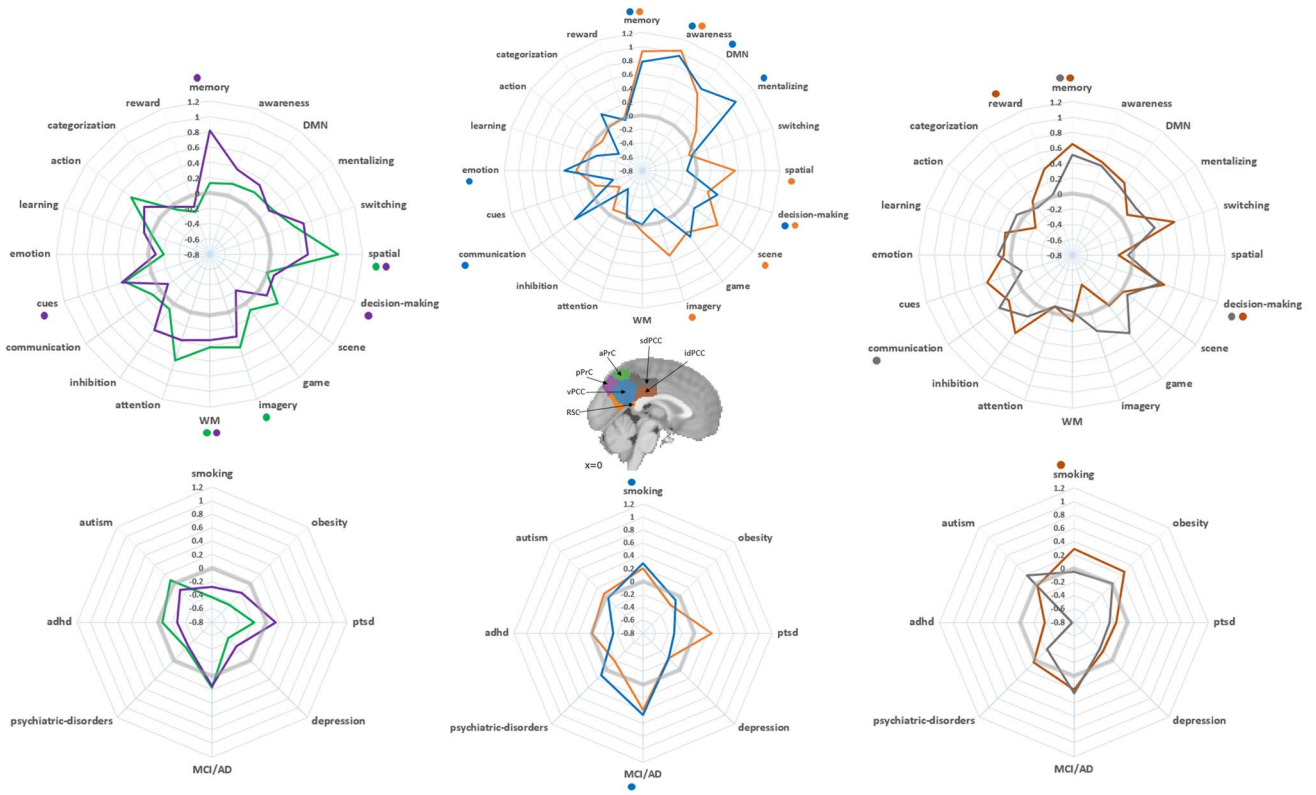

Fig. 11 Summary figure for the functional preference profiles of the whole PMC, with cognitive function-related topics in the top row and disorder-related topics in the bottom row. Cluster names/shapes included in the center for reference. See Figs. 3, 4 and 5 for detailed results

(Kobayashi and Amaral 2007), which are important areas for memory. Also, previous studies indicate a role of areas in PMC in conscious awareness (Stamatakis et al. 2010; Guldenmund et al. 2012; Adapa et al. 2014). Results from the coactivation map also showed that RSC had greater coactivation with parahippocampal cortex and vPCC showed greater coactivation with the temporal lobe. In addition to the association with 'memory', vPCC also showed associations with 'MCI/AD', which severely impact memory-related functions. This association is consistent with previous reports about the importance of PCC in amyloid deposition with Alzheimer's disease and performance on an episodic memory retrieval task in MCI (Ries et al. 2006; Sperling et al. 2009). Furthermore, the locations of amyloid deposition and fMRI activity in both studies are noticeably centered in vPCC. Although RSC did not show significant association with MCI/AD or DMN in whole PMC analysis, a recent paper does support the gateway function of RSC between the cortical DMN and medial temporal lobe structures (Kaboodvand et al. 2018), which are of pivotal importance in such disorders. That said, correlation of RSC in disorders featuring memory impairment might be more indirect or lateralized to one hemisphere, given that right RSC showed association with MCI/AD compared to left RSC in our lateralization analysis. This remains unclear, however, as our analysis showed that the 95% CI for the LOR was overlapping. VPCC also showed greater coactivation with bilateral TPJ and vmPFC compared to RSC, which are important DMN regions (Raichle et al. 2001; Buckner et al. 2008). Furthermore, vPCC showed the greatest correlation with 'mentalizing' among all clusters. Taken together with previous findings showing increased connectivity between the DMN and vPCC during internally focused states (Leech et al. 2011, 2012), vPCC can be seen as the one of the central hubs of the DMN. This helps to explain our present results, which show that vPCC is the only cluster significantly associated with 'DMN'.

Conclusions and future directions

Although our study provided a comprehensive analysis of the functional parcellation in PMC, there are some caveats worth addressing as well as questions for future research. First, none of the clusters yielded a single functional preference as the multivariate classifier used in this study is poor in its ability to predict activation by just using one (i.e., the strongest) associated topic. However, this might simply reflect the reality that no single brain region is associated with only a single function. Furthermore, like many other

multivariate models, the model we used in this study modeled the relationship between functional topics and activity purely with linear correlations, which necessarily ignores potential non-linear relationships (de la Vega et al. 2016, 2017).

Second, Neurosynth is an automated text-mining based dataset. Coordinates and terms were both extracted using an automated parser. Even though the topic modeling method remediated the redundancy and ambiguity issues caused by this term-based searching approach, researchers might have already introduced bias by describing conceptual terms they would like to address instead of actual behavioral or functional terms. Unlike Neurosynth, which works at the study level, the BrainMap dataset works at the experiment level (single contrast) with a set of labels predefined by experts (Laird et al. 2005, 2011). Since these two datasets show complementary limitations and advantages, it makes sense to combine them in a future study to provide a more comprehensive insight of functional profiles (Genon et al. 2018).

Third, even though the functional clusters showed some resemblance to anatomical organization, our clusters still had some overlap with different cytoarchitectonic regions. For example, the cluster we defined as RSC actually extended dorsally and posteriorly into part of PCC and precuneus. Also, our vPCC cluster did not separate into superior and inferior vPCC as defined in previous literature (Vogt 2009). Therefore, when interpreting the clusters generated using this method, we need to stress function over structure.

Fourth, in the functional lateralization analysis, one thing to note is that the PMC mask is based on the Harvard–Oxford anatomical atlas. Among other things, this means that the left and right PMC masks are not identical: the matrix of left PMC [4117 × 151,527] is smaller than that of right PMC [5248 × 151,527]. This might cause biases toward the larger matrix while comparing the functional preference profiles between left and right PMC.

This study presents a functional parcellation of PMC generated by a relatively unbiased data-driven approach. Our results support the idea that, as a single union, PMC supports different cognitive and disorder-related functions. As a brain region composed of sub-regions, different adjacent sub-regions in PMC share some functions in addition to their distinct functions. Our functional lateralization analysis also found some interesting results such as the possible lateralization effect of RSC in 'MCI/AD'. The present results can serve as a foundation for future, more fine-grained research as well as provide a functional parcellation to the poorly understood PMC.

Acknowledgements Research by Sven Vanneste and Yuefeng Huang was supported by the Defense Advanced Research Projects Agency (DARPA) Biological Technologies Office (BTO) TNT program under the auspices of Dr. Doug Weber and Tristan McClure-Begley through the Space and Naval Warfare Systems Center, Pacific Grant/Contract no. N66001-17-2-4011. Research by Sven Vanneste was also supported by Darrell Royal Foundation. Research by Jeffrey Hullfish was supported by the Eugene McDermott Graduate Fellowship (201501). The authors would like to thank Alejandro de la Vega for his help troubleshooting the code via email correspondence and his thoughtful comments on an earlier version of this manuscript.

Compliance with ethical standards

Conflict of interest The authors declare no competing financial interests. Code and data are available freely at https://github.com/adelavega/neurosynth-mfc and https://github.com/adelavega/neurosynth-lfc. Permissions (https://github.com/adelavega/neurosynth-mfc/blob/master/LICENSE and https://github.com/adelavega/neurosynth-lfc/blob/master/LICENSE) are granted to replicate these analyses on any given brain region at any desired spatial granularity. This material has not been peer reviewed.

References

Adapa RM, Davis MH, Stamatakis EA, Absalom AR, Menon DK (2014) Neural correlates of successful semantic processing during propofol sedation. Hum Brain Map 35(7):2935–2949. https://doi.org/10.1002/hbm.22375

Addis DR, Wong AT, Schacter DL (2007) Remembering the past and imagining the future: common and distinct neural substrates during event construction and elaboration. Neuropsychologia 45(7):1363–1377. https://doi.org/10.1016/j.neuropsychologia.2006.10.016

Buckner RL, Andrews-Hanna JR, Schacter DL (2008) The brain's default network: anatomy, function, and relevance to disease. Ann N Y Acad Sci 1124:1–38. https://doi.org/10.1196/annals.1440.011

Bzdok D, Heeger A, Langner R, Laird AR, Fox PT, Palomero-Gallagher N, Vogt BA, Zilles K, Eickhoff SB (2015) Subspecialization in the human posterior medial cortex. Neuroimage 106:55–71. https://doi.org/10.1016/j.neuroimage.2014.11.009

Cauda F, Geminiani G, D'Agata F, Sacco K, Duca S, Bagshaw AP, Cavanna AE (2010) Functional connectivity of the posteromedial cortex. PLoS One. https://doi.org/10.1371/journal.pone.0013107

Cavanna AE, Trimble MR (2006) The precuneus: a review of its functional anatomy and behavioural correlates. Brain 129(Pt 3):564–583. https://doi.org/10.1093/brain/awl004

David M. Blei AYN, Michael I. Jordan (2003) Latent dirichlet allocation. J Mach Learn Res 3:993–1022

de la Vega A, Chang LJ, Banich MT, Wager TD, Yarkoni T (2016) Large-scale meta-analysis of human medial frontal cortex reveals tripartite functional organization. J Neurosci 36(24):6553–6562. https://doi.org/10.1523/JNEUROSCI.4402-15.2016

de la Vega A, Yarkoni T, Wager TD, Banich MT (2017) Large-scale meta-analysis suggests low regional modularity in lateral frontal cortex. Cereb Cortex:1–15. https://doi.org/10.1093/cercor/bhx204

Desikan RS, Segonne F, Fischl B, Quinn BT, Dickerson BC, Blacker D, Buckner RL, Dale AM, Maguire RP, Hyman BT, Albert MS, Killiany RJ (2006) An automated labeling system for subdividing the human cerebral cortex on MRI scans into gyral based regions of interest. Neuroimage 31(3):968–980. https://doi.org/10.1016/j.neuroimage.2006.01.021

Dixon ML, De La Vega A, Mills C, Andrews-Hanna J, Spreng RN, Cole MW, Christoff K (2018) Heterogeneity within the frontoparietal control network and its relationship to the default and dorsal attention networks. Proc Natl Acad Sci. https://doi.org/10.1073/pnas.1715766115

Eickhoff SB, Thirion B, Varoquaux G, Bzdok D (2015) Connectivity-based parcellation: critique and implications. Hum Brain Map 36(12):4771–4792. https://doi.org/10.1002/hbm.22933

Fransson P (2006) How default is the default mode of brain function? Further evidence from intrinsic BOLD signal fluctuations. Neuropsychologia 44(14):2836–2845. https://doi.org/10.1016/j.neuropsychologia.2006.06.017

Genon S, Reid A, Langner R, Amunts K, Eickhoff SB (2018) How to characterize the function of a brain region. Trends Cogn Sci. https://doi.org/10.1016/j.tics.2018.01.010

Greicius MD, Srivastava G, Reiss AL, Menon V (2004) Default-mode network activity distinguishes Alzheimer's disease from healthy aging: evidence from functional MRI. Proc Natl Acad Sci USA 101(13):4637–4642. https://doi.org/10.1073/pnas.0308627101

Greicius MD, Supekar K, Menon V, Dougherty RF (2009) Resting-state functional connectivity reflects structural connectivity in the default mode network. Cereb Cortex 19(1):72–78. https://doi.org/10.1093/cercor/bhn059

Guldenmund P, Vanhaudenhuyse A, Boly M, Laureys S, Soddu A (2012) A default mode of brain function in altered states of consciousness. Archives italiennes de biologie 150(2–3):107–121. https://doi.org/10.4449/aib.v150i2.1373

Hampson M, Driesen N, Roth JK, Gore JC, Constable RT (2010) Functional connectivity between task-positive and task-negative brain areas and its relation to working memory performance. Magn Reson Imaging 28(8):1051–1057. https://doi.org/10.1016/j.mri.2010.03.021

Huang Y, Mohan A, De Ridder D, Sunaert S, Vanneste S (2018) The neural correlates of the unified percept of alcohol-related craving: a fMRI and EEG study. Sci Rep 8(1):923. https://doi.org/10.1038/s41598-017-18471-y

Huijbers W, Vannini P, Sperling RA, C MP, Cabeza R, Daselaar SM (2012) Explaining the encoding/retrieval flip: memory-related deactivations and activations in the posteromedial cortex. Neuropsychologia 50(14):3764–3774. https://doi.org/10.1016/j.neuropsychologia.2012.08.021

Kaboodvand N, Backman L, Nyberg L, Salami A (2018) The retrosplenial cortex: a memory gateway between the cortical default mode network and the medial temporal lobe. Hum Brain Map. https://doi.org/10.1002/hbm.23983

Karnath HO, Perenin MT (2005) Cortical control of visually guided reaching: evidence from patients with optic ataxia. Cereb Cortex 15(10):1561–1569. https://doi.org/10.1093/cercor/bhi034

Kobayashi Y, Amaral DG (2007) Macaque monkey retrosplenial cortex: III. Cortical efferents. J Comp Neurol 502(5):810–833. https://doi.org/10.1002/cne.21346

Krieger-Redwood K, Jefferies E, Karapanagiotidis T, Seymour R, Nunes A, Ang JWA, Majernikova V, Mollo G, Smallwood J (2016) Down but not out in posterior cingulate cortex: deactivation yet functional coupling with prefrontal cortex during demanding semantic cognition. Neuroimage 141:366–377. https://doi.org/10.1016/j.neuroimage.2016.07.060

Kunishio K, Haber SN (1994) Primate cingulostriatal projection: limbic striatal versus sensorimotor striatal input. J Comp Neurol 350(3):337–356. https://doi.org/10.1002/cne.903500302

Laird AR, Lancaster JL, Fox PT (2005) BrainMap: the social evolution of a human brain mapping database. Neuroinformatics 3(1):65–78

Laird AR, Eickhoff SB, Fox PM, Uecker AM, Ray KL, Saenz JJ Jr, McKay DR, Bzdok D, Laird RW, Robinson JL, Turner JA, Turkeltaub PE, Lancaster JL, Fox PT (2011) The BrainMap strategy for standardization, sharing, and meta-analysis of neuroimaging data. BMC Res Notes 4:349. https://doi.org/10.1186/1756-0500-4-349

Leech R, Sharp DJ (2014) The role of the posterior cingulate cortex in cognition and disease. Brain 137(Pt 1):12–32. https://doi.org/10.1093/brain/awt162

Leech R, Kamourieh S, Beckmann CF, Sharp DJ (2011) Fractionating the default mode network: distinct contributions of the ventral and dorsal posterior cingulate cortex to cognitive control. J Neurosci 31(9):3217–3224. https://doi.org/10.1523/JNEUROSCI.5626-10.2011

Leech R, Braga R, Sharp DJ (2012) Echoes of the brain within the posterior cingulate cortex. J Neurosci 32(1):215–222. https://doi.org/10.1523/JNEUROSCI.3689-11.2012

Luber B, Kinnunen LH, Rakitin BC, Ellsasser R, Stern Y, Lisanby SH (2007) Facilitation of performance in a working memory task with rTMS stimulation of the precuneus: frequency- and time-dependent effects. Brain Res 1128(1):120–129. https://doi.org/10.1016/j.brainres.2006.10.011

Maguire EA (2001) The retrosplenial contribution to human navigation: a review of lesion and neuroimaging findings. Scand J Psychol 42(3):225–238

Margulies DS, Smallwood J (2017) Converging evidence for the role of transmodal cortex in cognition. Proc Natl Acad Sci USA 114(48):12641–12643. https://doi.org/10.1073/pnas.1717374114

Margulies DS, Ghosh SS, Goulas A, Falkiewicz M, Huntenburg JM, Langs G, Bezgin G, Eickhoff SB, Castellanos FX, Petrides M, Jefferies E, Smallwood J (2016) Situating the default-mode network along a principal gradient of macroscale cortical organization. Proc Natl Acad Sci USA 113(44):12574–12579. https://doi.org/10.1073/pnas.1608282113

Mason MF, Norton MI, Van Horn JD, Wegner DM, Grafton ST, Macrae CN (2007) Wandering minds: the default network and stimulus-independent thought. Science 315(5810):393–395. https://doi.org/10.1126/science.1131295

Mazziotta JC, Toga AW, Evans A, Fox P, Lancaster J (1995) A probabilistic atlas of the human brain: theory and rationale for its development. ICBM Neuroimage 2(2):89–101

Osawa A, Maeshima S, Kubo K, Itakura T (2006) Neuropsychological deficits associated with a tumour in the posterior corpus callosum: a report of two cases. Brain Inj 20(6):673–676. https://doi.org/10.1080/02699050600676958

Palomero-Gallagher N, Eickhoff SB, Hoffstaedter F, Schleicher A, Mohlberg H, Vogt BA, Amunts K, Zilles K (2015) Functional organization of human subgenual cortical areas: relationship between architectonical segregation and connectional heterogeneity. Neuroimage 115:177–190. https://doi.org/10.1016/j.neuroimage.2015.04.053

Parvizi J, Van Hoesen GW, Buckwalter J, Damasio A (2006) Neural connections of the posteromedial cortex in the macaque. Proc Natl Acad Sci USA 103(5):1563–1568. https://doi.org/10.1073/pnas.0507729103

Pedregosa F, Varoquaux G, Gramfort A, Michel V, Thirion B, Grisel O, Blondel M, Prettenhofer P, Weiss R, Dubourg V, Vanderplas J, Passos A, Cournapeau D, Brucher M, Perrot M, Duchesnay É (2011) Scikit-learn: machine learning in Python. J Mach Learn Res 12:2825–2830

Raichle ME, MacLeod AM, Snyder AZ, Powers WJ, Gusnard DA, Shulman GL (2001) A default mode of brain function. Proc Natl Acad Sci USA 98(2):676–682. https://doi.org/10.1073/pnas.98.2.676

Ries ML, Schmitz TW, Kawahara TN, Torgerson BM, Trivedi MA, Johnson SC (2006) Task-dependent posterior cingulate activation in mild cognitive impairment. Neuroimage 29(2):485–492. https://doi.org/10.1016/j.neuroimage.2005.07.030

Romanski LM, Giguere M, Bates JF, Goldman-Rakic PS (1997) Topographic organization of medial pulvinar connections with the prefrontal cortex in the rhesus monkey. J Comp Neurol 379(3):313–332

Rudge P, Warrington EK (1991) Selective impairment of memory and visual perception in splenial tumours. Brain 114(Pt 1B):349–360

Shackman AJ, Salomons TV, Slagter HA, Fox AS, Winter JJ, Davidson RJ (2011) The integration of negative affect, pain and cognitive control in the cingulate cortex. Nat Rev Neurosci 12(3):154–167. https://doi.org/10.1038/nrn2994

Sperling RA, Laviolette PS, O'Keefe K, O'Brien J, Rentz DM, Pihlajamaki M, Marshall G, Hyman BT, Selkoe DJ, Hedden T, Buckner RL, Becker JA, Johnson KA (2009) Amyloid deposition is associated with impaired default network function in older persons without dementia. Neuron 63(2):178–188. https://doi.org/10.1016/j.neuron.2009.07.003

Stamatakis EA, Adapa RM, Absalom AR, Menon DK (2010) Changes in resting neural connectivity during propofol sedation. PLoS One 5(12):e14224. https://doi.org/10.1371/journal.pone.0014224

Vann SD, Aggleton JP, Maguire EA (2009) What does the retrosplenial cortex do? Nat Rev Neurosci 10(11):792–802. https://doi.org/10.1038/nrn2733

Vatansever D, Menon DK, Manktelow AE, Sahakian BJ, Stamatakis EA (2015) Default mode dynamics for global functional integration. J Neurosci 35(46):15254–15262. https://doi.org/10.1523/jneurosci.2135-15.2015

Vatansever D, Manktelow AE, Sahakian BJ, Menon DK, Stamatakis EA (2016) Cognitive flexibility: a default network and basal ganglia connectivity perspective. Brain Connect 6(3):201–207. https://doi.org/10.1089/brain.2015.0388

Vatansever D, Bzdok D, Wang HT, Mollo G, Sormaz M, Murphy C, Karapanagiotidis T, Smallwood J, Jefferies E (2017a) Varieties of semantic cognition revealed through simultaneous decomposition of intrinsic brain connectivity and behaviour. Neuroimage 158:1–11. https://doi.org/10.1016/j.neuroimage.2017.06.067

Vatansever D, Manktelow AE, Sahakian BJ, Menon DK, Stamatakis EA (2017b) Angular default mode network connectivity across working memory load. Hum Brain Map 38(1):41–52. https://doi.org/10.1002/hbm.23341

Vatansever D, Menon DK, Stamatakis EA (2017c) Default mode contributions to automated information processing. Proc Natl Acad Sci USA 114(48):12821–12826. https://doi.org/10.1073/pnas.1710521114

Vogt BA (2009) Cingulate neurobiology and disease. Oxford University Press, Oxford

Vogt BA, Pandya DN, Rosene DL (1987) Cingulate cortex of the rhesus monkey: I. Cytoarchitecture and thalamic afferents. J Comp Neurol 262(2):256–270. https://doi.org/10.1002/cne.902620207

Yarkoni T, Poldrack RA, Nichols TE, Van Essen DC, Wager TD (2011) Large-scale automated synthesis of human functional neuroimaging data. Nat Methods 8(8):665–670. https://doi.org/10.1038/nmeth.1635

Yeterian EH, Pandya DN (1988) Corticothalamic connections of paralimbic regions in the rhesus monkey. J Comp Neurol 269(1):130–146. https://doi.org/10.1002/cne.902690111